communications earth & environment

Article

https://doi.org/10.1038/s43247-024-01887-6

# Amplified threat of tropical cyclones to US offshore wind energy in a changing climate



Serena Lipari, Karthik Balaguru ✉, Julian Rice, Sha Feng, Wenwei Xu, Larry K. Berg & David Judi

The vulnerability of US offshore wind energy to tropical cyclones is a pressing concern, particularly along the Atlantic and Gulf Coasts, key areas for offshore wind energy development. Assessing the impact of projected climate change on tropical cyclones, and consequently on offshore wind resources, is thus critical for effective risk management. Herein, we investigate the evolving risk to offshore wind turbines posed by Atlantic tropical cyclones in a non-stationary climate using a synthetic tropical cyclone model. Integrated with climate model simulations, projections show widespread increases in tropical cyclone exposure, with historical 20-year storms occurring every ~12.7 years on average, increasing in intensity by about 9.3 $ms^{-1}$. Subsequent fragility analysis reveals that the probabilities of turbine yielding and buckling from a 20-year tropical cyclone could increase by about 37% and 13%, respectively, with regional increases reaching up to 51%. These findings carry substantial implications for the operation and future expansion of offshore wind farms.

Offshore wind (OSW) energy is poised to play a key role in achieving US renewable energy goals, with a national OSW energy target of 30 gigawatts (GW) by 2030[1]. This ambitious goal signals considerable growth in the wind energy sector over the coming decades, presenting substantial opportunities for OSW development along US coastal regions near major population centers[2]. In order to meet state and national energy goals, there are plans to establish wind energy areas (WEAs) along the US Atlantic and Gulf Coasts. However, these regions are susceptible to tropical cyclones (TCs), which have historically been among the most prevalent threats to life and property. Between 1980 and 2023, TCs impacting the US have caused over $1.3 trillion in damages, averaging $22.8 billion per event[3]. The potential for damage in coastal regions is expected to increase even further[4–10], with one study suggesting that the risk to people and property will rise by up to 60% by 2100[11]. With the projected expansion of OSW energy infrastructure along the Atlantic and Gulf Coasts, this underscores the need for more TC-resilient turbine designs and the consideration of TC hazards in wind farm siting plans.

To mitigate the damaging impacts of TCs on wind energy infrastructure, it is crucial for wind farm development plans to assess the risk to OSW turbines under extreme TC conditions. TCs are particularly impactful due to a combination of high wind speeds, heavy rainfall, and storm surges. Current theories and climate models predict that the intensity of storms and associated precipitation will increase in the future[12–20]. Although some studies suggest a decline in global TC frequency (TCF) under climate change[13,21–24], the interquartile range of outcomes from a number of studies spans positive change, indicating variability in the influence of warming on TCF[13]. Reports generally conclude that the proportion of storms reaching Categories 4 and 5 strength are expected to increase due to anthropogenic warming over the 21st century[13,20]. Moreover, future changes in steering flow may shift Atlantic TC tracks closer to the US coast[25,26], where environmental conditions are becoming increasingly favorable for TC intensification[27–31]. Thus, it is critical to understand the wind and wave impacts induced by TCs on wind turbines, particularly in coastal regions where TC impacts are expected to worsen.

Due to the lack of observed performance metrics for wind turbines during TCs, researchers commonly employ structural modeling techniques such as numerical finite element models, probabilistic models, and physics-based simulation tools[32–39]. Previous studies have developed extensive frameworks to quantify the risk posed by TCs to wind energy infrastructure, including assessments for offshore turbines in WEAs off the Atlantic and Gulf Coasts[36–38]. However, these studies did not consider potential changes in TC climatology due to future climate conditions. Therefore, there is an urgent need to understand the evolving TC risk to US OSW infrastructure through assessments that comprehensively account for changes in the climate system and their consequent impacts on storms.

To address this gap, we assess the impact of projected future changes in Atlantic TCs on US wind energy infrastructure using the Risk Analysis Framework for Tropical Cyclones (RAFT). RAFT is a hybrid model integrating physics, machine learning, and statistics, capable of generating large ensembles of TCs that are consistent with a given climate and achieve reasonable accuracy[25,40,41]. Specifically, we utilize turbine fragility curves[42] to simulate the structural response of fixed-bottom 5 megawatt (MW) OSW turbines along the US Atlantic and Gulf Coasts exposed to TC-induced wind and wave loadings based on RAFT-simulated TCs. Given that our study area

Pacific Northwest National Laboratory, Richland, WA, USA. ✉e-mail: karthik.balaguru@pnnl.gov

along the Atlantic and Gulf Coasts features shallow waters conducive to fixed-bottom turbines, we have focused our analysis on these structures. This focus on 5 MW turbines is motivated by the availability of fragility curves for the National Renewable Energy Laboratory's (NREL) 5 MW offshore reference turbine. While proposed US OSW turbines are expected to have higher capacities, the findings from this study can also provide indicative insights into the potential risks faced by these larger turbines. Our study not only evaluates how TC-induced risk to OSW infrastructure may change in the future, but also offers a novel methodology for risk assessment.

In our analysis, we will assess both overall TC exposure and risk patterns for the coastal region extending 200 km offshore from the Gulf and Atlantic Coasts, as well as subregional analyses (Northeast, Southeast, and Gulf) to investigate spatial variability in TC behavior and impacts between regions. Furthermore, we assess risk for specific WEAs at the state level (e.g., New York, North Carolina, and Texas) to allow for a more targeted analysis of the unique vulnerabilities in each region planning OSW energy development. This framework ensures a comprehensive assessment of OSW turbine risks under changing TC conditions, aiming to support the successful development of sustainable energy resources.

## Results

### Current and future wind turbine risk patterns

To relate TC wind speeds to the likelihood of turbine tower damage, we investigate two damage states: (a) yielding, which refers to permanent structural deformation, and (b) buckling, which refers to structural collapse. These states are determined via turbine fragility analysis, detailed further in the "Methods" section.

Using nine models from Phase 6 of the Coupled Model Intercomparison Project (CMIP6)[43] simulating historical (1980–2014) and future (2066–2100) climatic conditions under the SSP5-8.5 emissions scenario, we employed RAFT[40] to generate a combined total of 450,000 TC tracks within the Atlantic basin for each period, equivalent to nearly 60,000 years of total simulated TC activity. In addition to benefiting from a large sample of synthetic TCs that account for a range of climatic conditions, utilizing a model ensemble helps balance and reduce uncertainties from individual models[43,44], thereby enhancing the robustness of projections. For individual model output, see Section S2 of the Supplementary Information. Unless otherwise stated, the significance of projected changes is evaluated using two-tailed Student's *t*-tests at the 95% confidence level.

We investigate TC impacts using recurrence intervals or return periods (RPs), which provide a means to discern potential shifts in the occurrence rate of TCs of a particular intensity. Given that the average lifespan of a wind turbine is ~20 years[45–48], we assess the damage risk resulting from the peak wind speed associated with a 20-year RP TC (i.e., the TC with a 5% annual probability of occurrence) to evaluate the probabilities of yielding and buckling within a turbine's expected lifetime. Additionally, we repeat the analysis for a 50-year TC to assess the risk of more severe storms impacting the US Atlantic and Gulf Coasts.

Our findings indicate that the spatial risk of TC-induced damage to OSW turbines along the US Atlantic and Gulf Coast regions is broadly expected to increase, with strong intermodel agreement on the sign of change (i.e., increase or decrease) in all regions assessed. Detailed regional estimates and their associated uncertainties are outlined in Table 1. Significant increases in yielding risk are expected for the Gulf Coast and Florida peninsula resulting from 20- and 50-year storms (Fig. 1), with the average risk of turbine yielding estimated to increase by nearly 40% for a 20-year storm (Fig. 1c) and 27% for a 50-year storm (Fig. 1f). The Atlantic Coast exhibits similar changes, with projected increases in turbine yielding risk of about 35% for 20-year TCs and 31% for 50-year TCs.

Buckling, being a more acute damage state than yielding, requires higher wind speeds to surpass the structural limit. Historically, the probability that 20- or 50-year storms would induce turbine buckling has been below 10% across all regions assessed. However, under future climate change, this probability is estimated to rise to as high as 57% (Table 1), with the strongest increases and future risk expected for the Southeast and Gulf Coast regions (Fig. 2). For the Gulf Coast and Florida, buckling risk from a 20-year storm is projected to increase from nearly 0% to almost 18% (Fig. 2c). This increase is far more severe when considering a 50-year storm, with the buckling risk in this region expected to grow by almost a factor of eight. Along the Atlantic Coast, the likelihood of TC-induced turbine buckling is projected to rise as well, with anticipated increases in risk of about 9% for a 20-year TC and 34% for a 50-year TC. For both turbine yielding and buckling, the likelihood of damage is markedly higher for the Southeast than the Northeast, differing by almost 12% historically and by over 24% in a simulated future climate (Table 1).

### Tropical cyclone impacts on turbine risk

Our analysis indicates a substantial increase in TC-related risk to OSW turbines in the future, which prompts the question: Which underlying changes in storm climatology are responsible for these projected increases? To address this, we explore changes in TC climatology through two interconnected perspectives: shifting intensity distributions and changes in RPs of damaging storms.

RAFT achieves satisfactory performance against observations in capturing historical TC intensity along US coastal regions, with significant pixel-wise correlations of 0.74 for 20-year TCs and 0.81 for 50-year TCs (see Supplementary Information Section S1). Historically, 20-year TCs affecting US Atlantic and Gulf Coast WEAs have generally been approximately Category 1 storms (Fig. 3a). However, future 20-year TCs are anticipated to intensify to Category 2 storms, and even up to Category 3 storms in parts of the Gulf of Mexico (Fig. 3b). Concurrently, historical 50-year TCs have primarily been characterized by Categories 2 and 3 storms (Fig. 3d), while future projections show Category 4 storms dominating much of the Gulf and Atlantic offshore regions (Fig. 3e). For Florida and the Gulf Coast, average peak TC winds are estimated to increase by about 21–31% for 20- and 50-year storms (Fig. 3c, f), with similar changes projected for the Atlantic Coast, exhibiting increases of about 18–22%. Slightly stronger intensifications in peak TC wind speeds are expected for the Southeast compared to the Northeast, deviating by about 2 $ms^{-1}$ (Table 1).

Our results reveal that the RPs of storms with intensities commensurate with historical 20-year and 50-year TCs are forecasted to decrease, implying these intensities will become more frequent in the future. Specifically, storms with the intensity of historical 20-year TCs are estimated to occur every 12.7 years on average in the future (Table 1). Similarly, 50-year TCs are projected to occur nearly twice as often under future climatic conditions, impacting the Atlantic and Gulf Coasts roughly every 27.3 years.

Increases in the frequency of TCs making landfall also contribute to rising risks for coastal regions. Historically, about 27% of Atlantic TCs ($\geq$18 $ms^{-1}$) simulated with RAFT make US landfall, comparable to the observed rate of ~25% (Supplementary Information Section S1). This is projected to increase to 34 ± 4% in a future climate based upon TC simulations forced by nine distinct CMIP6 models. When considering only Categories 1–5 TCs ($\geq$33 $ms^{-1}$), the results indicate an increase from nearly 14% historically to 20 ± 3% in the future. Overall, changes in the landfall of Categories 1–5 TCs along the Gulf Coast and Florida are higher than for the Atlantic Coast, with average increases of 5 ± 3% for the former compared to 2 ± 1% for the latter. Furthermore, significant increases are expected in Category 4 storms across all regions, along with a rise in the most severe Category 5 TCs for the Southeast and Gulf Coasts (Table 2). These increases in coastal TCF are consistent with findings for the Atlantic basin under historical and projected future climatic conditions based upon a similar methodology[25], wherein substantial increases in track density appear to span nearly the entire coastal region, supporting our findings of increased TC landfall rates and broad elevated exposure of TCs to OSW turbines.

Wind speeds associated with turbine tower yielding generally correspond to Categories 2 and 3 TCs, while the more severe Categories 4 and 5 TCs are linked to high probabilities of turbine buckling (Supplementary Fig. S7). These associations are based on our fragility analysis, detailed in the "Methods" section. Specifically considering TC wind speeds associated with

**Table 1 | Offshore wind turbine risk and tropical cyclone intensity across US regions under historical and future climate scenarios**

| Region | | Yielding risk (%) | | Buckling risk (%) | | TC intensity ($ms^{-1}$) | | Return period (years) |
|---|---|---|---|---|---|---|---|---|
| | | Historical | Future | Historical | Future | Historical | Future | Future |
| Northeast | 20y RP | 2.4 ± 0.9 | 28.2 ± 5.1 | 0.01 ± 0.01 | 3.1 ± 1 | 36.5 ± 1 | 43.3 ± 1.3* | 11.8 ± 1** |
| | 50y RP | 24.9 ± 4.6 | 60.6 ± 6* | 0.9 ± 0.3 | 21.1 ± 4 | 44.2 ± 0.9 | 51.3 ± 1.2* | 22.7 ± 2.9** |
| Southeast | 20y RP | 7.3 ± 2.1 | 52.4 ± 7.1* | 0.09 ± 0.04 | 15.5 ± 3.6 | 39.8 ± 1.1 | 48.7 ± 1.6* | 12.2 ± 1.3** |
| | 50y RP | 58.4 ± 6.1 | 85.5 ± 4.7* | 9 ± 2.1 | 57.2 ± 6.3* | 50.2 ± 1 | 59.3 ± 1.4** | 24.5 ± 3.8** |
| Gulf | 20y RP | 1.8 ± 0.3 | 41.2 ± 2.8** | 0.01 ± 0.01 | 17.5 ± 1.7** | 34.4 ± 0.7 | 45.1 ± 1.1* | 13.3 ± 1.5** |
| | 50y RP | 54.1 ± 2.9 | 81.3 ± 2.9** | 7.3 ± 0.7 | 57.4 ± 3** | 48.9 ± 0.7 | 58.9 ± 1.1* | 30.4 ± 8.6** |
| Overall | 20y RP | 3 ± 0.5 | 40 ± 2.5** | 0.03 ± 0.01 | 13.4 ± 1.3** | 36 ± 0.5 | 45.3 ± 0.8** | 12.7 ± 0.8** |
| | 50y RP | 47.4 ± 2.5 | 76.8 ± 2.5** | 6 ± 0.6 | 48 ± 2.6** | 47.9 ± 0.5 | 57 ± 0.8** | 27.3 ± 3.9** |

Ensemble mean values are shown for offshore turbine risk and peak tropical cyclone intensity associated with 20- and 50-year RP storms. Risk reflects the likelihood of the specified storm intensity inducing each damage state. The rightmost column presents the projected future return periods for wind speeds corresponding to historical 20- and 50-year RP storms. Confidence intervals are constructed at the 95% confidence level using ensemble mean data. Future values marked with a (*) indicate statistically significant increases at the 90% confidence level, while (**) denotes significance at the 95% confidence level. Values <0.1 are reported with an additional significant digit.

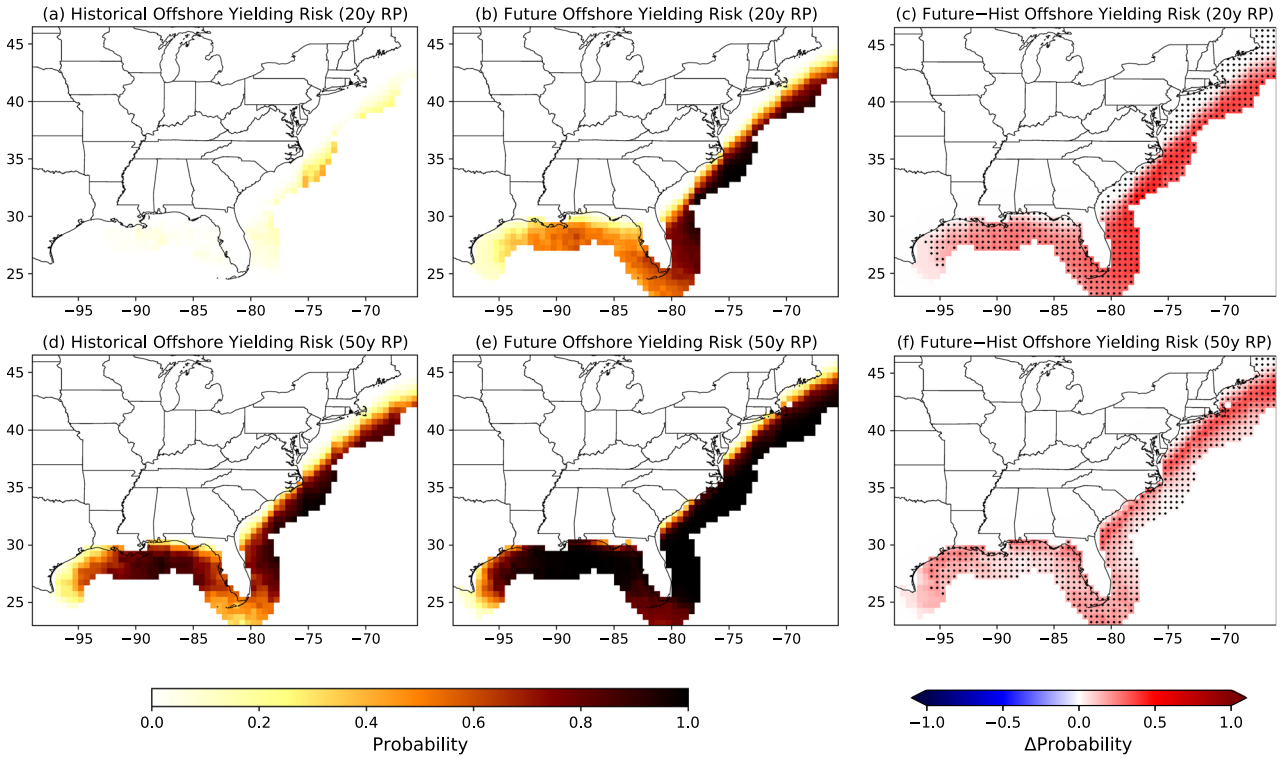


**Fig. 1 | Offshore turbine tower yielding probabilities under different tropical cyclone intensities.** Probabilities represent the likelihood of towers beginning to yield due to exposure to tropical cyclone winds for historical (1980–2014) and future (2066–2100) periods. **a**, **d** Historical yielding probabilities for 20-year and 50-year tropical cyclones, respectively. **b**, **e** Future yielding probabilities for 20-year and 50-year tropical cyclones. **c**, **f** Difference (future minus historical) in yielding probabilities for 20-year and 50-year tropical cyclones. Black markers denote regions where at least 8 out of 9 models agree on the sign of the difference.

tower yielding and buckling, we find that yielding-inducing winds are expected to increase in frequency within the study area by about 56 ± 4% on average, while the frequency of TC wind speeds associated with turbine buckling are projected to rise by a factor of ~3 (Table 2). Higher variability in the frequency of yielding-inducing winds is observed for the Atlantic Coast compared to the Gulf Coast, a trend illustrated at the state level for New York, North Carolina, and Texas in Fig. 4, each of which has an OSW pipeline capacity of at least 3 GW[49].

Assessing changes in yielding and buckling wind frequency at the state level allows for a more targeted analysis of the unique vulnerabilities in each region planning OSW energy development. The results indicate a general upward shift in the frequency distribution of damaging winds, particularly those associated with catastrophic turbine damage. The Northeast region is expected to experience the largest increase in the study area, with the frequency of buckling-inducing winds growing by nearly a factor of five, as exemplified for New York WEAs in Fig. 4. North Carolina WEAs exhibit the highest exposure among the three states assessed, with a nearly threefold higher frequency of buckling-inducing winds compared to those in offshore regions of New York. Texas WEAs are subjected to the lowest degree of variability in exposure of these states, projected however to face pointed increases in the frequency of buckling winds. These state-level changes align with the broader regional trends outlined in Table 2, which details the

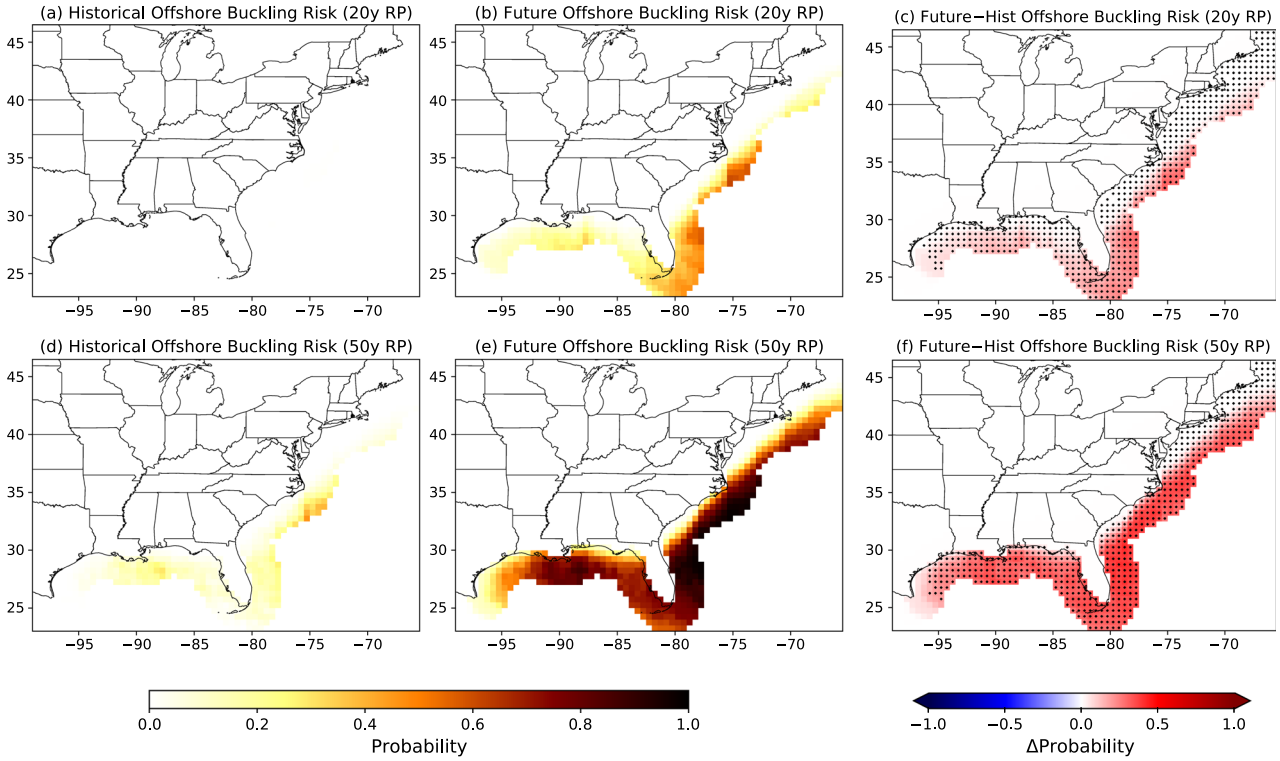


**Fig. 2 | Offshore turbine tower buckling probabilities under different tropical cyclone intensities.** Probabilities represent the likelihood of tower buckling (i.e., collapse) due to exposure to tropical cyclone winds for historical (1980–2014) and future (2066–2100) periods. **a**, **d** Historical buckling probabilities for 20-year and 50-year tropical cyclones, respectively. **b**, **e** Future buckling probabilities for 20-year and 50-year tropical cyclones. **c**, **f** Difference (future minus historical) in buckling probabilities for 20-year and 50-year tropical cyclones. Black markers denote regions where at least 8 out of 9 models agree on the sign of the difference.

frequency changes for Categories 1–5 TCs for the Northeast, Southeast, and Gulf regions.

## Discussion

This study introduces a novel framework for assessing the evolving TC risk to OSW turbines along the US Atlantic and Gulf Coasts, as outlined in Fig. 5. By utilizing historical and future global climate simulations with RAFT[40], we generated synthetic TCs and applied structural fragility functions specifically developed for OSW turbines[42] to translate TC wind speeds into damage risk.

Our analysis projects substantial increases in both the frequency and intensity of TCs in the future. While the IPCC Sixth Assessment Report forecasts with medium confidence a global decline or no change in the frequency of TC formation with increasing global warming[20], regional changes, particularly in the North Atlantic, remain uncertain and show conflicting results. For instance, Chand et al.[50] find both decreasing and increasing trends in North Atlantic TCF over different time periods. Considerable uncertainty remains in the projected impacts of climate change on TCF, largely due to internal climate variations and systematic intermodel differences in sea surface temperature (SST) responses to increasing greenhouse gases[13,50–53]. Although the Atlantic basin has seen increased TC activity since the 1970s, there continues to be debate over whether this trend is driven more by internal climatic variability or by anthropogenic forcing[13,50–58]. Crucially, our findings are consistent with other research predicting an escalation in the proportion of intense storms (Categories 4 and 5) as a consequence of global warming[13,15,18], driven by rising SSTs and a more thermodynamically favorable environment[59–63]. These estimates also broadly agree with previous studies suggesting an increased likelihood of US landfall under global warming due to changing SST patterns and steering flow[25,26,64,65].

Analyses performed here are based on a CMIP6 multimodel ensemble average, which reduces potential biases inherent in individual models[43,44]. Combined with the improved consensus among CMIP6 models regarding future ocean warming patterns compared to CMIP5[25], this strengthens the reliability of the climate projections we use to downscale TC activity. The findings presented here are substantial, yet it is important to note that climate-induced changes in TCs remain a dynamic and evolving research area, with ongoing advancements in both TC theory and the simulation capabilities of global climate models (GCMs) (e.g., refs. 4,10,13,21,24,25,51,57,66–71). While the accuracy of TC intensity and frequency projections is expected to improve, RAFT demonstrates robust performance in replicating historical TC behavior[40], thereby enhancing the credibility of our study (see Supplementary Information Section S1). Consequently, this substantiates our findings of increased TC intensity and frequency, thereby underpinning the elevated risk to OSW turbines.

The overall variability in turbine damage is influenced by various site-specific factors such as turbine design and ocean depth[72]. Climatological differences, such as the SST front associated with the Gulf Stream, also play a significant role in TC behavior. The sharp gradient in risk along the Atlantic Coast can partly be attributed to this SST front[73], as observed in both our results (e.g., Fig. 1b, d), and in observed TCs (Supplementary Fig. S3). The findings of this study hold considerable implications for the planning and development of WEAs and OSW infrastructure. To mitigate heightened TC risks, it is crucial to strategically site turbines in lower-risk areas and to enhance design standards to withstand more intense TCs, thereby ensuring the sustainability and resilience of renewable energy infrastructure in the face of escalating TC threats. The need for region-specific mitigation strategies is underscored by the spatial variability identified here, with the likelihood of turbine buckling estimated to be 2–5× larger for the Southeast coastal region compared to the Northeast (Table 1). Moreover, increased TC risks are anticipated for onshore wind infrastructure, particularly in coastal regions of New England, North Carolina, and Gulf Coast states (Supplementary Fig. S9), as well as in Puerto Rico, where substantial increases in TC activity and subsequent turbine damage risk are expected (Supplementary

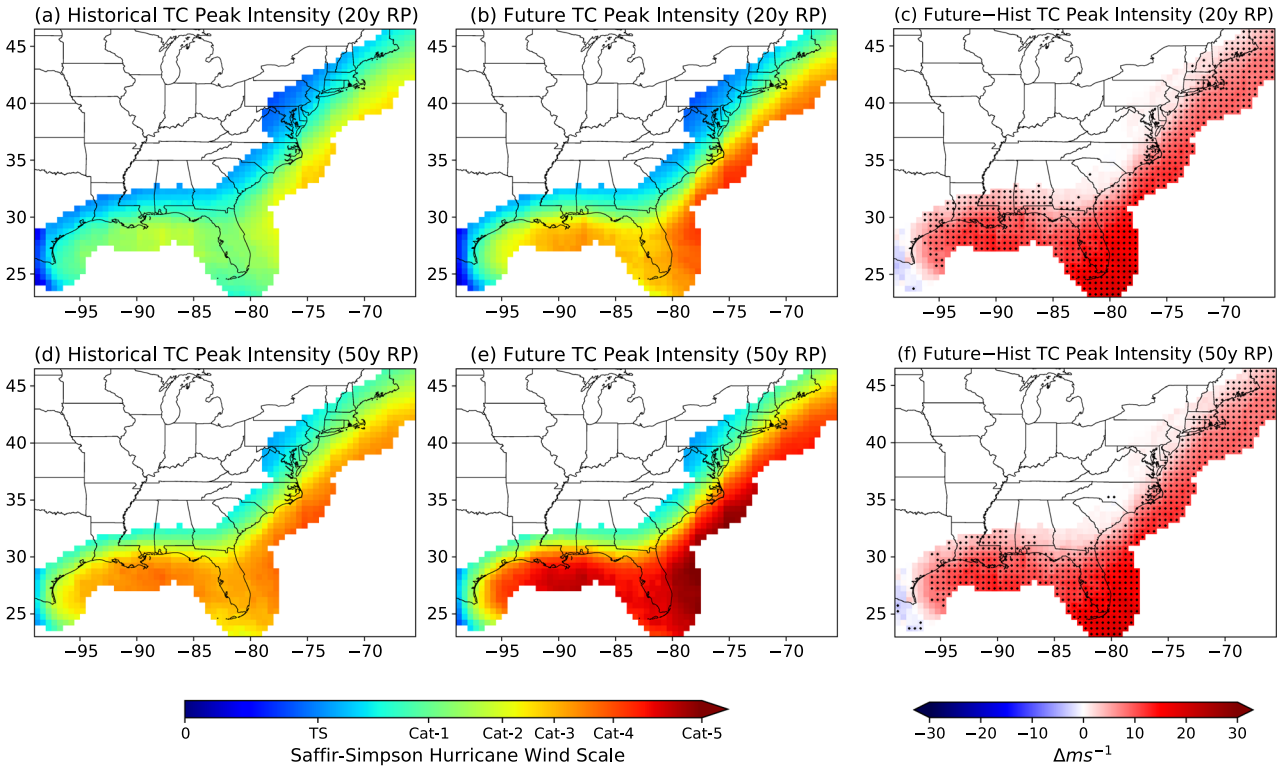


**Fig. 3 | Maximum sustained 1-min hub height (90 m) tropical cyclone wind speeds.** Return period wind speeds are computed assuming 14.91 events per year, based on the exceedance probability distribution of tropical cyclones passing through each 0.5° × 0.5° pixel. **a**, **d** Historical (1980–2014) wind speeds for 20-year and 50-year tropical cyclones, respectively. **b**, **e** Future (2066–2100) wind speeds for 20-year and 50-year tropical cyclones. **c**, **f** Difference (future minus historical) in wind speeds for 20-year and 50-year tropical cyclones. Regions with black markers denote areas where at least 8 out of 9 models agree on the sign of the difference.

**Table 2 | Tropical cyclone track density across US regions under historical and future climate scenarios**

| TC Frequency (per square 5 degrees, per 50,000 TCs) | | | | | | |
|---|---|---|---|---|---|---|
| **Region** | | **Cat-1** | **Cat-2** | **Cat-3** | **Cat-4** | **Cat-5** |
| Northeast | Historical | 10,707 ± 1646 | 4271 ± 773 | 2126 ± 385 | 525 ± 122 | 3 ± 1 |
| | Future | 12,350 ± 1931 | 7211 ± 1145* | 4781 ± 796* | 2624 ± 493** | 255 ± 56 |
| Southeast | Historical | 3996 ± 705 | 2029 ± 388 | 1463 ± 273 | 861 ± 153 | 104 ± 24 |
| | Future | 4835 ± 841* | 2762 ± 521* | 2441 ± 493* | 2292 ± 473** | 768 ± 153** |
| Gulf | Historical | 2480 ± 237 | 1407 ± 141 | 1209 ± 121 | 817 ± 79 | 225 ± 25 |
| | Future | 3105 ± 287* | 1779 ± 173* | 1736 ± 162* | 2070 ± 205** | 1214 ± 130** |
| Overall | Historical | 3977 ± 378 | 1950 ± 164 | 1396 ± 126 | 787 ± 68 | 185 ± 19 |
| | Future | 4794 ± 386 | 2763 ± 237* | 2324 ± 180* | 2199 ± 200** | 976 ± 99** |

Track density is computed per square 5 degrees by summing and aggregating occurrences within each 0.5 × 0.5 degree subregion for every 50,000 Atlantic tropical cyclones, based on the ensemble mean from nine models. Confidence intervals are constructed at the 95% confidence level via bootstrapping with 1000 samples. Future values marked with a (*) indicate statistically significant increases at the 90% confidence level, while (**) denotes significance at the 95% confidence level. Note that the frequency data includes multiple observations of the same storm as it traverses regions.

Fig. S10). Detailed discussions on onshore TC risk can be found in Section S4 of the Supplementary Information.

Additionally, the risk analysis methodology we utilized faces uncertainties due to the lack of empirical performance metrics for large-scale OSW turbines subjected to extreme TC conditions[38]. Our fragility analysis is based upon the NREL 5 MW offshore reference turbine[74], whereas proposed OSW turbines in the study regions may range between 11–15 MW[49]. Notably, two of the three currently operational offshore projects in the US utilize 6 MW turbines, which closely align with our 5 MW baseline, thus justifying our choice[75]. It is important to recognize that along with other elements of turbine design, differences in turbine capacities can affect their vulnerability to wind and wave loadings. Moreover, the fragility functions applied here are extrapolated from operational wind speeds to higher magnitudes associated with TCs. Despite these uncertainties, using an alternative fragility function[36] calibrated for TC-force wind speeds yielded similar broad-scale conclusions for turbine buckling risk, affirming the robustness of our results (see Supplementary Information Section S3).

The absence of detailed fragility analyses along with the anticipated intensification of TCs highlights the urgent need to address these gaps and implement effective mitigation strategies. Protecting OSW turbines from the increasing TC threat due to climate change involves measures such as improved siting protocols and enhanced design standards. These steps are critical to ensuring the long-term sustainability and resilience of the renewable energy sector.

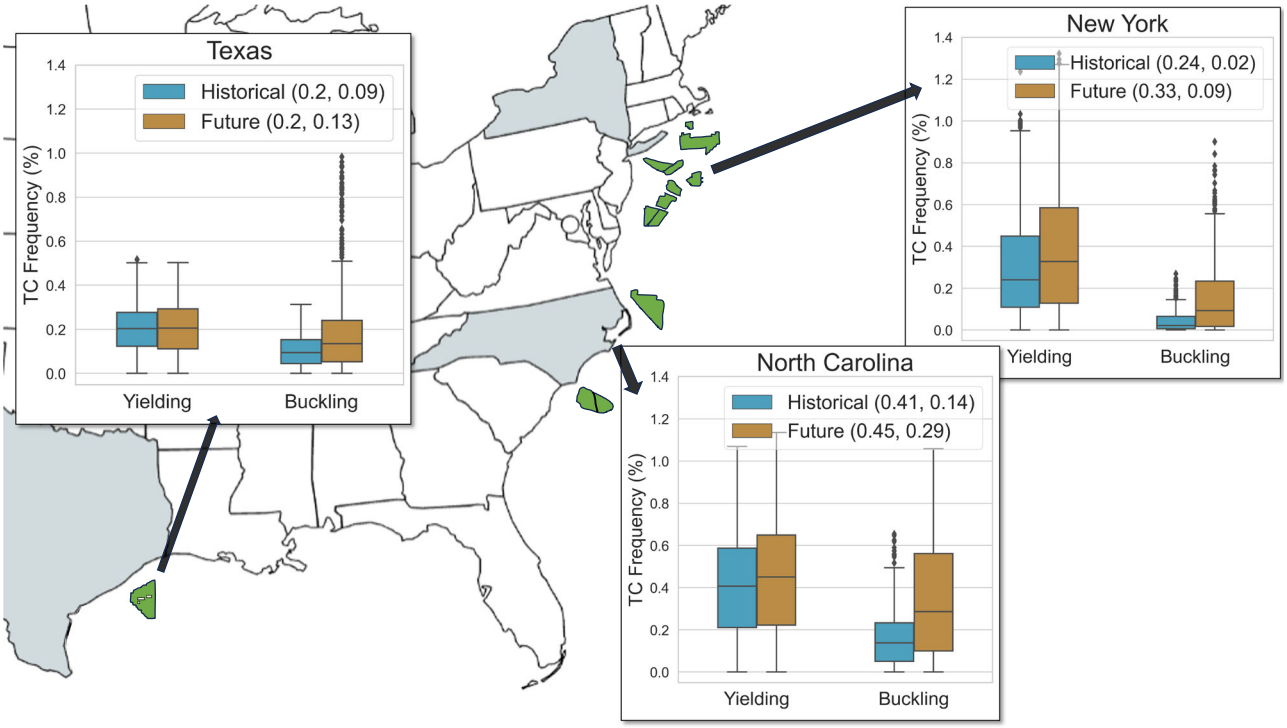


**Fig. 4 | Frequency distributions of tropical cyclone winds leading to turbine yielding and buckling in selected US wind energy areas (WEAs).** WEAs are depicted for New York, North Carolina, and Texas, based on the 2023 Offshore Wind Market Report[49]. Distributions are derived from storms simulated under historical (1980–2014) and future (2066–2100) climates using data from nine CMIP6 climate models. Percentages are calculated as the average tropical cyclone track density within each 0.5° × 0.5° grid cell for each region, relative to all simulated landfalling tropical cyclones for each period. The legend provides the 50th percentile frequency percentages for yielding and buckling, respectively. Differences shown are significant at the 99% confidence level using two-tailed Student's *t*-tests. WEAs are assigned to states based on existing power offtake contracts but may be reallocated; they are not depicted to scale.

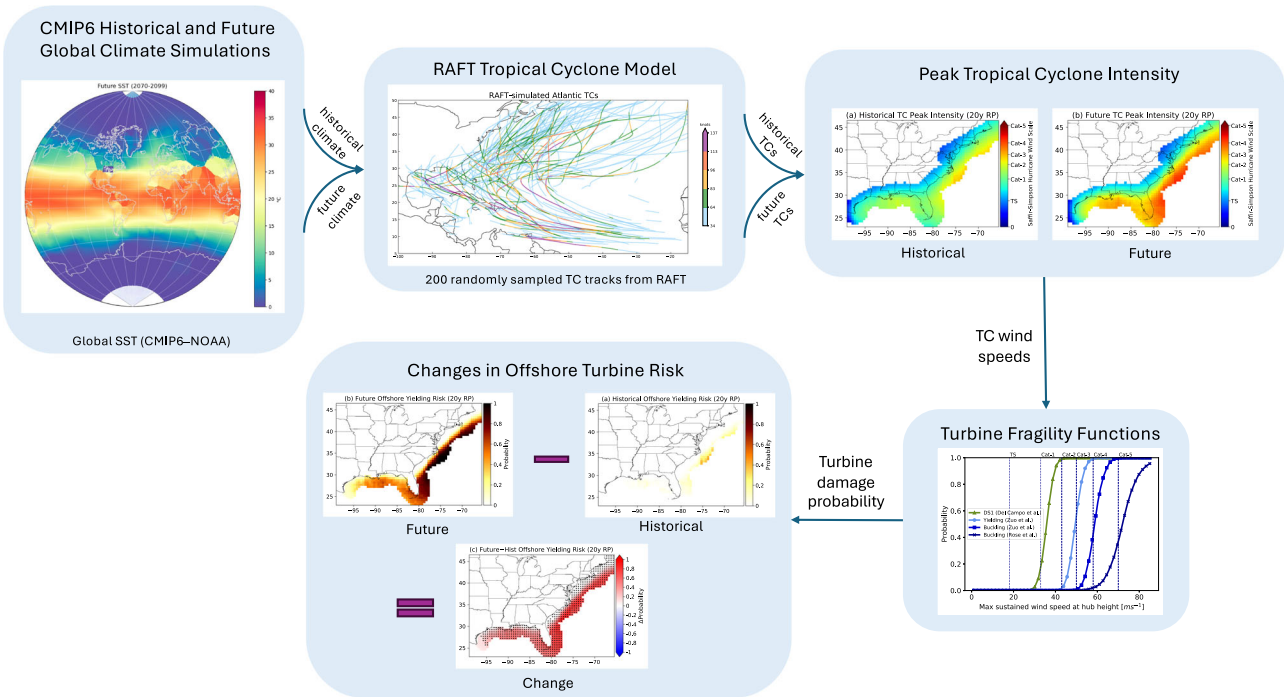


**Fig. 5 | Workflow for offshore wind turbine risk assessment.** This study's workflow begins with the use of a multimodel ensemble from CMIP6 to simulate global environmental conditions, generating tropical cyclones with RAFT for historical and future periods. The sustained peak intensity of these tropical cyclones is then utilized to apply turbine fragility functions, mapping wind speeds to damage risks associated with wind and wave forcing. This process produces spatial maps of offshore wind turbine risk for both periods, which are subsequently used to assess the projected change in damage likelihood under a high-emissions future climate.

## Methods

### Tropical cyclone simulations

To represent environmental conditions for historical and future climates, we utilize a multimodel ensemble of nine fully coupled GCMs from CMIP6: Euro-Mediterranean Centre on Climate Change-coupled climate model (CMCC-CM2-SR5), Canadian Earth System Model (CanESM5), Energy Exascale Earth System Model (E3SM), EC-Earth Consortium Model (EC-Earth3), Geophysical Fluid Dynamics Laboratory Climate Model (GFDLCM4), Institute Pierre Simon Laplace Climate Model (IPSL-CM6A-LR), Model for Interdisciplinary Research on Climate (MIROC6), Max Planck Institute Earth System Model (MPI-ESM1-2-LR), and Meteorological Research Institute Earth System Model (MRI-ESM2-0). These models were selected based on the availability of data for historical (1980–2014) and future periods (2066–2100) under the SSP5-8.5 emissions scenario[43] as well as a sensitivity analysis indicating that these models are broadly representative of the CMIP6 multimodel ensemble[25].

As illustrated in Fig. 5, we employed the hybrid RAFT model to generate 50,000 synthetic TCs in the Atlantic basin, forced by climatic conditions from each of the nine CMIP6 models for each time period[40]. RAFT consists of a track model which determines storm movement through the basin as governed by large-scale wind patterns, and an intensity model that predicts storm strength based on the environmental conditions encountered along the track. The RAFT model employs a variety of input variables, including large-scale wind, relative humidity, wind shear, maximum potential intensity, equivalent potential temperature, and surface roughness, to generate synthetic TCs. Historical and future TC intensities simulated by RAFT are bias-corrected using quantile delta mapping[66,76] to improve the reliability of RAFT TCs in representing observed TC behavior. This bias correction modifies the RAFT-modeled TC intensities by aligning the quantiles of the historical data with those of the observed records, and then this same correction is applied to projected intensities ensuring a more accurate representation of TC behavior and enhancing the model's predictive reliability. Compared to best-track observations from the International Best Track Archive for Climate Stewardship (IBTrACS)[77], RAFT effectively captures the spatial distribution of both TC tracks and peak intensity for 20- and 50-year storms. We find significant pixel-wise correlations between RAFT simulations and observations when comparing historical maximum sustained (10-min mean) TC wind speeds offshore, with Pearson $r$-squared values of 0.89 and 0.96 along with mean relative errors of 0.12 and 0.03 for 20- and 50-year storms, respectively. Further model validation metrics and discussions are provided in Section S1 of the Supplementary Information.

For each model, maximum sustained 10 meter TC wind speeds were recorded during both historical and future periods and then converted to hub height (90 m) wind speeds using the mean eyewall wind profile[78]. Once hub height wind speeds were determined, 20- and 50-year TC wind speeds were calculated using a pixel-wise ($0.5 \times 0.5$ degree cell) RP computation. TC wind speeds were ranked by intensity within each spatial grid cell, and using the observed annual average of 14.91 storms per year (from 1980 to 2014), we determined the wind speed corresponding to specific RPs. RPs were calculated as the inverse probability of an event of at least a given magnitude occurring in any year. The 20- and 50-year RP storms were then computed for historical and future climates simulated by each of the nine models, and an ensemble mean was taken across each spatial grid cell to produce the wind speed maps illustrated in Fig. 3.

For our risk assessment, we selected an offshore area within 200 km of the coast to balance proximity to existing wind farms, typically located within 150 km of the shore, with the potential for future wind farm development extending across the Outer Continental Shelf. According to the 2024 edition of the Offshore Wind Market Report, current draft WEAs extend beyond 150 km offshore[75]. A sensitivity analysis indicated a similar likelihood of TC risk when limiting the domain to within 150 km of the coast, with approximately a 10.6% lower damage risk resulting from 20- and 50-year TCs in the nearshore region. This consideration allows our analysis to be pertinent for assessing near-term risk and informing the ongoing identification of optimal wind energy locations under future climate conditions.

### Tropical cyclone frequency analysis

To further understand the frequency distribution of TCs in different regions impacted by Atlantic TCs, we segmented the study area into three regions based on latitudinal ranges: the Northeast (38°N, 46.5°N], Southeast [31°N, 38°N], and Gulf [22.5°N, 31°N). Each region was divided into square 5° subregions, within which we analyzed TC track data to tally the number of TCs of each intensity category (e.g., Categories 1–5) passing through each $0.5° \times 0.5°$ grid cell.

For each $0.5° \times 0.5°$ grid cell, we recorded the frequency of TCs by intensity category and aggregated the data at the regional level to create comprehensive frequency distributions representing TC track density. This frequency analysis was based on simulations of 50,000 TCs per subregion for both historical and future climate scenarios. This allowed us to derive the average frequency of TCs by intensity category for each region, consequently providing insights into the regional shifts in TC climatology. Aggregated results were utilized to calculate the average track density of TCs of each intensity per region, reflecting the total frequency based on the 50,000 TCs per $5° \times 5°$ subregion.

Landfall events were identified by counting instances where the center of a TC crossed within 30 km of the US coastline. Using the RAFT model ensemble, we derived the 95% confidence interval for the simulated mean landfall proportion to account for intermodel variability in landfall patterns. To validate the landfall frequency of TCs, we compared historical RAFT-simulated TCs with all pre-2015 historical observations from IBTrACS. Figure S1a, b of the Supplementary Information details simulated and observed TCF distribution across the Atlantic basin, supporting the landfall frequency analysis and providing context for the broader spatial patterns of TCs. The calculated validation statistics, including the mean TCF values, correlation coefficient, and mean absolute error are provided in Section S1 of the Supplementary Information.

### Fragility analysis

Several studies have extensively analyzed the dynamic behaviors of wind turbines under various sources of vibration, such as aerodynamic forces, sea waves, and seismic loadings [e.g.,[33–35,79,80]]. To simplify computations, turbines are often considered in a parked condition with the mass of the blades lumped at the top of the tower[42]. The parked condition is realistic for assessing TC risk to wind turbines because the conventional cut-out wind speed for turbines of 25 $ms^{-1}$ is well below wind speeds associated with even Category 1 TCs[81].

Risk assessment for wind turbines due to aerodynamic forcing is typically modeled using a log-logistic or log-normal distribution[34,36,38,42,82], which maps wind speed to the probability of damage or malfunction. The parameters for these models are determined using wind turbine structural simulations subjected to external forces. Many analyses, including this study, are based upon the NREL 5 MW offshore baseline wind turbine (with a 90 m hub height) because its properties are well-documented and publicly available[74].

Damage states relate the structural performance of wind turbines to their displacement response under external forcings, such as aerodynamic and sea wave loadings. The turbine tower begins to yield when the internal stress response to forced displacement becomes nonlinear. For the turbine assessed here, yielding is estimated to occur when the displacement at the top of the turbine tower reaches 2.1 m, determined through pushover analysis[42]. A top-of-tower displacement of about 2.9 m is associated with turbine tower buckling, characterized by sudden collapse or structural failure.

Once turbine structural damage states are defined, fragility functions are used to estimate the probability of exceeding the associated displacement thresholds as a function of wind speed, depicted in Supplementary Fig. S7. For OSW risk assessment, we implement fragility functions for turbine tower yielding and buckling, which account for both wind and wave

loadings impacting a 5 MW non-yawing wind turbine[42]. While the wind speeds in that study are within the normal operating range of a turbine (3–25 $ms^{-1}$) and are unlikely to cause the major damage TCs can inflict, we assess more severe damage states from yielding- and buckling-inducing winds, which we find to range between Categories 2 and 5 TCs, with wind speeds from 43 $ms^{-1}$ to over 70 $ms^{-1}$ (Supplementary Fig. S7).

To investigate the sensitivity of our results to the choice of fragility function, we repeated the buckling risk analysis using an alternative method developed for OSW turbines[36] and found comparable results. Further details are provided in Section S3 of the Supplementary Information.

## Data availability

Damage probability maps from the turbine risk assessment performed in this study are available on the open-source repository Zenodo at https://zenodo.org/records/11130961[83]. Although the RAFT input data for this analysis is not yet published, RAFT-simulated TCs forced by ERA5 reanalysis are freely accessible at https://doi.org/10.5281/zenodo.10392723. Additionally, the CMIP6 global climate model data used for forcing TCs can be accessed at https://pcmdi.llnl.gov/CMIP6/.

## Code availability

Code for processing input data and implementing the turbine fragility function to generate probability maps is available upon reasonable request.

Received: 24 May 2024; Accepted: 7 November 2024;
Published online: 09 December 2024

## References

1. U.S. Department of Energy. Energy Secretary Granholm Announces Ambitious New 30GW Offshore Wind Deployment Target by 2030. https://www.energy.gov/articles/energy-secretary-granholm-announces-ambitious-new-30gw-offshore-wind-deployment-target (2021).
2. Veers, P. et al. Grand challenges in the science of wind energy. *Science* **366**, eaau2027 (2019).
3. Smith, A. *US Billion-Dollar Weather and Climate Disasters* (NOAA National Centers for Environmental Information (NCEI), 2018).
4. Mendelsohn, R., Emanuel, K., Chonabayashi, S. & Bakkensen, L. The impact of climate change on global tropical cyclone damage. *Nat. Clim. Change* **2**, 205–209 (2012).
5. Nordhaus, W. D. The economics of hurricanes and implications of global warming. *Clim. Change Econ.* **1**, 1–20 (2010).
6. Narita, D., Tol, R. S. & Anthoff, D. Damage costs of climate change through intensification of tropical cyclone activities: an application of fund. *Clim. Res.* **39**, 87–97 (2009).
7. Pielke Jr, R. A. Future economic damage from tropical cyclones: sensitivities to societal and climate changes. *Philos. Trans. R. Soc. A Math. Phys. Eng. Sci.* **365**, 2717–2729 (2007).
8. Bakkensen, L. A. & Mendelsohn, R. O. Global tropical cyclone damages and fatalities under climate change: an updated assessment. *Hurric. Risk* **1**, 179–197 (2019).
9. Schmidt, S., Kemfert, C. & Höppe, P. The impact of socio-economics and climate change on tropical cyclone losses in the USA. *Reg. Environ. Change* **10**, 13–26 (2010).
10. Dinan, T. Projected increases in hurricane damage in the United States: the role of climate change and coastal development. *Ecol. Econ.* **138**, 186–198 (2017).
11. Arkema, K. K. et al. Coastal habitats shield people and property from sea-level rise and storms. *Nat. Clim. Change* **3**, 913–918 (2013).
12. Knutson, T. R. et al. Dynamical downscaling projections of Twenty-First-Century Atlantic Hurricane Activity: CMIP3 and CMIP5 model-based scenarios. *J. Clim.* **26**, 6591–6617 (2013).
13. Knutson, T. et al. Tropical cyclones and climate change assessment: part II: projected response to anthropogenic warming. *Bull. Am. Meteorol. Soc.* **101**, E303–E322 (2020).
14. Wright, D. B., Knutson, T. R. & Smith, J. A. Regional climate model projections of rainfall from us landfalling tropical cyclones. *Clim. Dyn.* **45**, 3365–3379 (2015).
15. Kossin, J. P., Knapp, K. R., Olander, T. L. & Velden, C. S. Global increase in major tropical cyclone exceedance probability over the past four decades. *Proc. Natl Acad. Sci. USA* **117**, 11975–11980 (2020).
16. Emanuel, K. Increasing destructiveness of tropical cyclones over the past 30 years. *Nature* **436**, 686–688 (2005).
17. Patricola, C. M. & Wehner, M. F. Anthropogenic influences on major tropical cyclone events. *Nature* **563**, 339–346 (2018).
18. Elsner, J. B., Kossin, J. P. & Jagger, T. H. The increasing intensity of the strongest tropical cyclones. *Nature* **455**, 92–95 (2008).
19. Guzman, O. & Jiang, H. Global increase in tropical cyclone rain rate. *Nat. Commun.* **12**, 5344 (2021).
20. Seneviratne, S. I. et al. Weather and Climate Extreme Events in a Changing Climate. In *Climate Change 2021: The Physical Science Basis. Contribution of Working Group I to the Sixth Assessment Report of the Intergovernmental Panel on Climate Change* (eds Masson-Delmotte, V. et al.) (Cambridge University Press, 2021).
21. Chand, S. S. et al. Declining tropical cyclone frequency under global warming. *Nat. Clim. Change* **12**, 655–661 (2022).
22. Zhao, H. et al. Decreasing global tropical cyclone frequency in CMIP6 historical simulations. *Sci. Adv.* **10**, eadl2142 (2024).
23. Sugi, M. & Yoshimura, J. Decreasing trend of tropical cyclone frequency in 228-year high-resolution AGCM simulations. *Geophys. Res. Lett.* **39**, L19805 (2012).
24. Tory, K. J., Chand, S. S., McBride, J. L., Ye, H. & Dare, R. Projected changes in late-twenty-first-century tropical cyclone frequency in 13 coupled climate models from Phase 5 of the Coupled Model Intercomparison Project. *J. Clim.* **26**, 9946–9959 (2013).
25. Balaguru, K. et al. Increased US coastal hurricane risk under climate change. *Sci. Adv.* **9**, eadf0259 (2023).
26. Knutson, T. R., Sirutis, J. J., Bender, M. A., Tuleya, R. E. & Schenkel, B. A. Dynamical downscaling projections of late twenty-first-century us landfalling hurricane activity. *Clim. Change* **171**, 28 (2022).
27. Emanuel, K. Will global warming make hurricane forecasting more difficult? *Bull. Am. Meteorol. Soc.* **98**, 495–501 (2017).
28. Ting, M., Kossin, J. P., Camargo, S. J. & Li, C. Past and future hurricane intensity change along the US East Coast. *Sci. Rep.* **9**, 7795 (2019).
29. Balaguru, K. et al. Increasing hurricane intensification rate near the US Atlantic Coast. *Geophys. Res. Lett.* **49**, e2022GL099793 (2022).
30. Li, Y. et al. Recent increases in tropical cyclone rapid intensification events in global offshore regions. *Nat. Commun.* **14**, 5167 (2023).
31. Garner, A. J. Observed increases in North Atlantic tropical cyclone peak intensification rates. *Sci. Rep.* **13**, 16299 (2023).
32. Jonkman, J. M. & Buhl, M. L. *Fast User's Guide* (National Renewable Energy Laboratory, Golden, CO, 2005).
33. Zuo, H., Bi, K. & Hao, H. Dynamic analyses of operating offshore wind turbines including soil-structure interaction. *Eng. Struct.* **157**, 42–62 (2018).
34. Martin del Campo, J. O., Pozos-Estrada, A. & Pozos-Estrada, O. Development of fragility curves of land-based wind turbines with tuned mass dampers under cyclone and seismic loading. *Wind Energy* **24**, 737–753 (2021).
35. Mardfekri, M. & Gardoni, P. Multi-hazard reliability assessment of offshore wind turbines. *Wind Energy* **18**, 1433–1450 (2015).
36. Rose, S., Jaramillo, P., Small, M. J., Grossmann, I. & Apt, J. Quantifying the hurricane risk to offshore wind turbines. *Proc. Natl Acad. Sci. USA* **109**, 3247–3252 (2012).
37. Rose, S., Jaramillo, P., Small, M. J. & Apt, J. Quantifying the hurricane catastrophe risk to offshore wind power. *Risk Anal.* **33**, 2126–2141 (2013).

38. Hallowell, S. T. et al. Hurricane risk assessment of offshore wind turbines. *Renew. Energy* **125**, 234–249 (2018).
39. Bennett, J. A. et al. Extending energy system modelling to include extreme weather risks and application to hurricane events in Puerto Rico. *Nat. Energy* **6**, 240–249 (2021).
40. Xu, W. et al. A North Atlantic synthetic tropical cyclone track, intensity, and rainfall dataset. *Sci. Data* **11**, 130 (2024).
41. Xu, W. et al. Deep learning experiments for tropical cyclone intensity forecasts. *Weather Forecast.* **36**, 1453–1470 (2021).
42. Zuo, H. et al. Fragility analyses of offshore wind turbines subjected to aerodynamic and sea wave loadings. *Renew. Energy* **160**, 1269–1282 (2020).
43. O'Neill, B. C. et al. The Scenario Model Intercomparison Project (ScenarioMIP) for CMIP6. *Geosci. Model Dev.* **9**, 3461–3482 (2016).
44. Lei, X. et al. Evaluation of CMIP6 models and multi-model ensemble for extreme precipitation over arid Central Asia. *Remote Sens.* **15**, 2376 (2023).
45. Liu, P. & Barlow, C. Y. Wind turbine blade waste in 2050. *Waste Manag.* **62**, 229–240 (2017).
46. Gurzenich, D. & Mathur, J. *Material and Energy Demand for Selected Renewable Energy Technologies* (International Bureau of the BMBF, 1998).
47. Krohn, S. The energy balance of modern wind turbines. *Wind Power* **16**, 1–15 (1997).
48. Schleisner, L. Life cycle assessment of a wind farm and related externalities. *Renew. Energy* **20**, 279–288 (2000).
49. Musial, W. et al. *Offshore Wind Market Report: 2023 Edition* (National Renewable Energy Laboratory (NREL), Golden, CO, United States, 2023).
50. Chan, J. C. & Liu, K. S. Global warming and Western North Pacific typhoon activity from an observational perspective. *J. Clim.* **17**, 4590–4602 (2004).
51. Walsh, K. J. et al. Tropical cyclones and climate change. *Wiley Interdiscip. Rev. Clim. Change* **7**, 65–89 (2016).
52. Bhatia, K., Vecchi, G., Murakami, H., Underwood, S. & Kossin, J. Projected response of tropical cyclone intensity and intensification in a global climate model. *J. Clim.* **31**, 8281–8303 (2018).
53. Knutson, T. R., Sirutis, J. J., Garner, S. T., Held, I. M. & Tuleya, R. E. Simulation of the recent multidecadal increase of Atlantic hurricane activity using an 18-km-grid regional model. *Bull. Am. Meteorol. Soc.* **88**, 1549–1565 (2007).
54. Villarini, G., Vecchi, G. A., Knutson, T. R., Zhao, M. & Smith, J. A. North Atlantic tropical storm frequency response to anthropogenic forcing: projections and sources of uncertainty. *J. Clim.* **24**, 3224–3238 (2011).
55. Holland, G. J. & Webster, P. J. Heightened tropical cyclone activity in the North Atlantic: natural variability or climate trend? *Philos. Trans. R. Soc. A Math. Phys. Eng. Sci.* **365**, 2695–2716 (2007).
56. Bell, G. D. & Chelliah, M. Leading tropical modes associated with interannual and multidecadal fluctuations in North Atlantic hurricane activity. *J. Clim.* **19**, 590–612 (2006).
57. Mann, M. E. & Emanuel, K. A. Atlantic hurricane trends linked to climate change. *EOS Trans. Am. Geophys. Union* **87**, 233–241 (2006).
58. Landsea, C. W., Pielke Jr, R. A., Mestas-Nunez, A. M. & Knaff, J. A. Atlantic basin hurricanes: indices of climatic changes. *Clim. Change* **42**, 89–129 (1999).
59. Sobel, A. H. et al. Human influence on tropical cyclone intensity. *Science* **353**, 242–246 (2016).
60. Knutson, T. et al. Tropical cyclones and climate change assessment: part I: detection and attribution. *Bull. Am. Meteorol. Soc.* **100**, 1987–2007 (2019).
61. Kossin, J. P., Olander, T. L. & Knapp, K. R. Trend analysis with a new global record of tropical cyclone intensity. *J. Clim.* **26**, 9960–9976 (2013).
62. Emanuel, K. A statistical analysis of tropical cyclone intensity. *Mon. Weather Rev.* **128**, 1139–1152 (2000).
63. Wehner, M. F. & Kossin, J. P. The growing inadequacy of an open-ended Saffir–Simpson hurricane wind scale in a warming world. *Proc. Natl Acad. Sci. USA* **121**, e2308901121 (2024).
64. Dailey, P. S., Zuba, G., Ljung, G., Dima, I. M. & Guin, J. On the relationship between North Atlantic Sea surface temperatures and US Hurricane Landfall Risk. *J. Appl. Meteorol. Climatol.* **48**, 111–129 (2009).
65. Garner, A. J., Kopp, R. E. & Horton, B. P. Evolving tropical cyclone tracks in the North Atlantic in a warming climate. *Earth's Future* **9**, e2021EF002326 (2021).
66. Gori, A., Lin, N., Xi, D. & Emanuel, K. Tropical cyclone climatology change greatly exacerbates US extreme rainfall–surge hazard. *Nat. Clim. Change* **12**, 171–178 (2022).
67. Knutson, T. R. et al. Tropical cyclones and climate change. *Nat. Geosci.* **3**, 157–163 (2010).
68. Druyan, L. M., Lonergan, P. & Eichler, T. A GCM investigation of global warming impacts relevant to tropical cyclone genesis. *Int. J. Climatol. J. R. Meteorol. Soc.* **19**, 607–617 (1999).
69. Zhao, M. & Held, I. M. Tc-permitting GCM simulations of hurricane frequency response to sea surface temperature anomalies projected for the late-twenty-first century. *J. Clim.* **25**, 2995–3009 (2012).
70. Murakami, H. & Wang, B. Patterns and frequency of projected future tropical cyclone genesis are governed by dynamic effects. *Commun. Earth Environ.* **3**, 77 (2022).
71. Ramsay, H. A., Singh, M. S. & Chavas, D. R. Response of tropical cyclone formation and intensification rates to climate warming in idealized simulations. *J. Adv. Model. Earth Syst.* **12**, e2020MS002086 (2020).
72. Hallowell, S. & Myers, A. Site-specific variability of load extremes of offshore wind turbines exposed to hurricane risk and breaking waves. *Wind Energy* **20**, 143–157 (2017).
73. Jones, E., Parfitt, R., Wing, A. A. & Hart, R. Gulf stream sea surface temperature anomalies associated with the extratropical transition of North Atlantic tropical cyclones. *Geophys. Res. Lett.* **50**, e2023GL102904 (2023).
74. Jonkman, J., Butterfield, S., Musial, W. & Scott, G. *Definition of a 5-MW Reference Wind Turbine for Offshore System Development* (National Renewable Energy Laboratory (NREL), Golden, CO, United States, 2009).
75. McCoy, A. et al. *Offshore Wind Market Report: 2024 Edition* (National Renewable Energy Laboratory (NREL), Golden, CO, United States, 2024).
76. Cannon, A. J., Sobie, S. R. & Murdock, T. Q. Bias correction of GCM precipitation by quantile mapping: how well do methods preserve changes in quantiles and extremes? *J. Clim.* **28**, 6938–6959 (2015).
77. Knapp, K. R., Kruk, M. C., Levinson, D. H., Diamond, H. J. & Neumann, C. J. The International Best Track Archive for Climate Stewardship (IBTrACS) unifying tropical cyclone data. *Bull. Am. Meteorol. Soc.* **91**, 363–376 (2010).
78. Franklin, J. L., Black, M. L. & Valde, K. Eyewall wind profiles in hurricanes determined by GPS dropwindsondes. Preprints, *24th Conference on Hurricanes and Tropical Meteorology,* 446–447 (American Meteorological Society, 2000).
79. Asareh, M.-A., Schonberg, W. & Volz, J. Effects of seismic and aerodynamic load interaction on structural dynamic response of multi-megawatt utility scale horizontal axis wind turbines. *Renew. Energy* **86**, 49–58 (2016).
80. Katsanos, E. I., Sanz, A. A., Georgakis, C. T. & Thöns, S. Multi-hazard response analysis of a 5MW offshore wind turbine. *Procedia Eng.* **199**, 3206–3211 (2017).
81. Bortolotti, P. et al. *IEA Wind TCP Task 37: Systems Engineering in Wind Energy-WP2. 1 Reference Wind Turbines* (National Renewable Energy Laboratory (NREL), 2019).

82. Li, C., Li, H.-N., Hao, H., Bi, K. & Chen, B. Seismic fragility analyses of sea-crossing cable-stayed bridges subjected to multi-support ground motions on offshore sites. *Eng. Struct.* **165**, 441–456 (2018).
83. Lipari, S. et al. Offshore wind turbine damage probability maps and hub height TC wind speeds for U.S. Atlantic and Gulf Coasts exposed to historical and future tropical cyclones *Data set. Zenodo.* (2024).

## Acknowledgements

This research was supported by the U.S. Department of Energy (DOE) Office of Science Biological and Environmental Research as part of the collaborative, multiprogram Integrated Coastal Modeling (ICoM) project. This work was also funded by the U.S. DOE, Office of Energy Efficiency and Renewable Energy, and Wind Energy Technologies Office (WETO). The research used computational resources from the National Energy Research Scientific Computing Center (NERSC), a U.S. DOE User Facility supported by the Office of Science under contract DE-AC02-05CH11231. For CMIP5 and CMIP6, the U.S. DOE's Program for Climate Model Diagnostics and Intercomparison provides coordinating support and leads the development of software infrastructure in partnership with the Global Organization for Earth System Science Portals. We acknowledge the World Climate Research Program's Working Group on Coupled Modeling, which is responsible for CMIP5 and CMIP6, and thank the climate modeling groups for producing and making available the model output. The Pacific Northwest National Laboratory is operated for DOE by Battelle Memorial Institute under contract DE-AC05-76RL01830.

## Author contributions

K.B., S.F., L.B., and D.J. conceptualized the research. K.B., S.F., S.L., and J.R. designed the methodology. S.L. conducted the literature review. W.X., K.B., and J.R. generated the input data. S.L. performed the formal analysis, validation, and visualization. J.R. supported model implementation. S.L., K.B., J.R., and S.F. contributed to investigation and interpretation. S.L. and K.B. drafted the paper. All authors contributed to revising the manuscript.

## Competing interests

The authors declare no competing interests.

## Additional information

**Supplementary information** The online version contains supplementary material available at https://doi.org/10.1038/s43247-024-01887-6.

**Correspondence** and requests for materials should be addressed to Karthik Balaguru.

**Peer review information** *Communications Earth & Environment* thanks Naveed Akhtar and the other, anonymous, reviewer(s) for their contribution to the peer review of this work. Primary Handling Editors: Olusegun Dada and Alireza Bahadori. A peer review file is available.